J|A|C|S
ARTICLES
Published on Web 11/27/2003

Sensitive High Resolution Inverse Detection NMR Spectroscopy of Proteins in the Solid State

Eric K. Paulson,[†] Corey R. Morcombe,[†] Vadim Gaponenko,[‡] Barbara Dancheck,[‡] R. Andrew Byrd,[‡] and Kurt W. Zilm*[,†]

Contribution from the Department of Chemistry, Yale University, P.O. Box 208107, New Haven, Connecticut 06520-8107, and the Structural Biophysics Laboratory, National Cancer Institute, Frederick, Maryland 21702

Received July 16, 2003; E-mail: kurt.zilm@yale.edu

Abstract: A new indirect detection scheme for obtaining $^{15}N/^{1}H$ shift correlation spectra in crystalline proteins is described. Excellent water suppression is achieved without the need for pulsed field gradients, and using only a 2-step phase cycle. Careful attention to overall NMR instrument stability was found critical for obtaining the best resolution and sensitivity. Magnetic dilution by deuteration of the protein in combination with high-speed magic angle spinning produces ^{1}H resonances averaging only 0.22 ppm in width, and in some cases lines as narrow as 0.17 ppm are obtained. In application to two different polymorphs of ubiquitin, structure dependent differences in both ^{15}N and ^{1}H amide chemical shifts are observed. In one case, distinct shifts for different molecules in the asymmetric unit are seen, and all differ substantially from solution NMR shifts. A gain of 7 in sensitivity makes the method competitive with solution NMR as long as nanocrystalline samples are available.

Introduction

Whereas the chemistry of proteins is most often studied in fluid solution phase, their structures are more often studied as frozen crystals. The two main characterization tools employed, solution phase NMR and X-ray crystallography, provide complementary windows on their chemistry, structure and dynamics. Solid state NMR (ssNMR) is uniquely positioned to relate crystallographic and fluid phase NMR data and to address important questions in biophysical chemistry. Macromolecular systems too insoluble for liquid state NMR or too disordered for X-ray crystallography can often be most profitably studied using ssNMR methods.

One of the primary impediments to wide adoption of ssNMR as a biophysical tool for studying large molecules has been insufficient sensitivity in comparison to solution NMR. This is largely a result of the fact that ssNMR methods almost universally rely on detection of nuclei such as ^{13}C or ^{15}N, which readily provide narrow lines and a high degree of dispersion in chemical shift. In solution NMR, it has long been recognized that indirect detection of the heteronuclei via the sample's protons[1] can provide a significant increase in sensitivity by virtue of the much higher ^{1}H gyromagnetic ratio γ. Even with this recognition and the experimental demonstration of the sensitivity advantage in model systems,[2−5] indirect detection of ^{13}C and ^{15}N nuclei via ^{1}H has only very recently been applied to NMR spectroscopy of a small protein.[6] In this paper, we present a new ssNMR indirect detection method, which in comparison has superior sensitivity, an 8-fold shorter phase cycle, and does not require pulsed field gradients (pfgs) for water suppression. Using this method, we demonstrate that high quality $^{15}N/^{1}H$ heteronuclear single quantum coherence (HSQC) spectra can be obtained with 500 nanomoles of nanocrystalline ubiquitin in less than 15 min on a modern 800 MHz NMR instrument. These results are achieved by a combination of careful attention to instrument stability, pulse sequence design, and sample preparation. Average ^{1}H line widths of only 0.22 ppm full width at half-maximum (fwhm) are observed. We also for the first time observe distinct ^{1}H and ^{15}N amide chemical shifts for magnetically inequivalent copies of the same protein in the asymmetric unit, and for different crystal polymorphs of the same protein.

Sensitivity in Indirect Detection

There are a number of approaches to calculating the signal-to-noise gain in ^{1}H versus X nucleus detection.[3,5] We follow Hoult and use the reciprocity principle.[7,8] This can be used to directly relate the efficiency in detection to the efficiency in excitation rather than the coil Q. The latter can be difficult to determine, whereas the radio frequency field (RF) amplitude B_{1w} normalized for unit input power[7] is readily measured. If

[†] Department of Chemistry, Yale University.
[‡] Structural Biophysics Laboratory, National Cancer Institute.

(1) Maudsley, A. A.; Muller, L.; Ernst, R. R. *J. Magn. Reson.* **1977**, *28*, 463−469.
(2) Ishii, Y.; Tycko, R. *J. Magn. Reson.* **2000**, *142*, 199−204.
(3) Ishii, Y.; Yesinowski, J. P.; Tycko, R. *J. Am. Chem. Soc.* **2001**, *123*, 2921−2922.
(4) Hong, M.; Yamaguchi, S. *J. Magn. Reson.* **2001**, *150*, 43−48.
(5) Reif, B.; Griffin, R. G. *J. Magn. Reson.* **2003**, *160*, 78−83.
(6) Chevelkov, V.; van Rossum, B. J.; Castellani, F.; Rehbein, K.; Diehl, A.; Hohwy, M.; Steuernagel, S.; Engelke, F.; Oschkinat, H.; Reif, B. *J. Am. Chem. Soc.* **2003**, *125*, 7788−7789.
(7) Hoult, D. I.; Richards, R. E. *J. Magn. Reson.* **1976**, *24*, 71−85.
(8) Hoult, D. I. *Concepts Magn. Reson.* **2000**, *12*, 173−187.

polarization transfer is used to equalize the ^{1}H and X nuclei differential spin populations, the ratio of signal voltages ξ_H/ξ_X following cross polarization for equal numbers of spins then is simply

$$\frac{\xi_H}{\xi_X} = \frac{\gamma_H^2(B_{1w})_H}{\gamma_X^2(B_{1w})_X} \quad (1)$$

Assuming t_1 and t_2 are set to $\sim 3T_2$ to provide the same resolution in both experiments, the only additional factors to take into account are the relative line widths $\nu_{1/2}$, and the fractional efficiency f of the additional magnetization transfer required in all indirect detection schemes. For a fixed number of total scans, the indirect-to-direct relative signal-to-noise ratio for a slice in the 2D spectrum is

$$\frac{(S/N)_H}{(S/N)_X} = f\frac{\gamma_H^2(B_{1w})_H}{\gamma_X{}^2(B_{1w})_X}\sqrt{\frac{(\nu_{1/2})_X}{(\nu_{1/2})_H}} \quad (2)$$

This ratio is appropriate for a balanced single coil multiple resonance probe where the ^{1}H and X nucleus RF fields are relatively homogeneous across the sample, and ^{1}H and X nucleus receiver channels have equal noise figures. In our experiments X is ^{15}N, and the ^{1}H operating frequency is 800 MHz. The triple resonance probe[9] used has a ratio $(B_{1w})_H/(B_{1w})_X = 0.36$. With a short cross polarization (CP) of 150 μs for the magnetization transfer step, the maximum value for f is measured by us to be 0.45. The gain in sensitivity then hinges on the line widths, and the ratio for our experimental situation then in theory is

$$\frac{(S/N)_H}{(S/N)_N} = 16.2 \times \sqrt{\frac{(\nu_{1/2})_N}{(\nu_{1/2})_H}} \quad (3)$$

This last equation emphasizes how critical the relative line widths are in terms of the real achievable sensitivity advantage. Every factor of 2 reduction in ^{1}H line width results in a factor of $\sqrt{2}$ higher signal-to-noise. However, it is also possible to give the illusion of achieving a sensitivity gain by simply doing a poor job on the X nucleus, for instance by less than optimal ^{1}H decoupling.

^{1}H Line Narrowing Strategy

Given the importance of achieving the narrowest ^{1}H line widths, we have made an in-depth comparison of several approaches. This work will be reported on in full at a later date and is similar in scope to that recently reported in a study using the α-spectrin SH3 domain as the test sample.[6] However, the results are described now in conjunction with the present work as they are quite different in many aspects. These differences most likely stem from the fact that our work has been carried out at a ^{1}H operating frequency of 800 MHz and utilized magic angle spinning (MAS) at 20 kHz, whereas the prior study utilized 500 MHz ^{1}H operation and 10 kHz MAS.

^{15}N and ^{1}H detected ^{15}N/^{1}H correlation spectra have been compared for both ^{15}N enriched and perdeuterated ^{15}N enriched ubiquitin prepared in two different nanocrystalline forms. The latter sample provides fully protonated amides diluted in a perdeuterated matrix by crystallization from normal aqueous media. Proton line narrowing was compared for MAS alone or with frequency switched Lee-Goldburg (FSLG) [10−12] decoupling, both with and without magnetic dilution.[13] In brief, we find that ^{15}N detected ^{15}N/^{1}H correlation spectra using FSLG ^{1}H line narrowing have close to the same line widths on a ppm scale in both perprotio and perdeutero protein. This indicates that MAS alone provides sufficient deuteron dipolar decoupling, and that the strength of the ^{1}H−^{1}H dipolar couplings is not the limiting factor in reducing the FSLG line widths. A comparison of the ^{1}H line widths obtained with either FSLG or MAS alone on perdeutero protein finds them equivalent in ppm once the 0.58 FSLG scaling factor is accounted for. This observation would suggest that the line widths are close to being limited by the effective ^{1}H T_2, and are scaled according to the fraction of time the spins effectively spend evolving in the transverse plane as expressed by the scaling factor. Application of low level WALTZ-16 ^{15}N decoupling during ^{1}H evolution[5] improves the ^{1}H line shape in all instances. Unfortunately, X nucleus decoupling during t_1 in X nucleus detect FSLG experiments on model compounds is also accompanied by a significant increase in t_1 noise. Presumably, this is caused by small amounts of cross polarization transfer[14] during decoupling.

The best combination of resolution and sensitivity in ^{1}H detect experiments is thus obtained with ^{15}N decoupling and MAS alone on perdeuterated samples. If we take line widths in Hz to directly reflect the spectrum obtained upon Fourier transform of the data,[15] the widths we observe for perdeuterated samples are the same when only FSLG is employed as when ^{15}N decoupling and only MAS is applied instead. Because FSLG decoupling scales the ^{1}H chemical shift interaction by a factor of 0.58, the lines must be narrowed with FSLG by more than a factor of 1.7 to achieve an increase in spectral resolution. Said another way, the ^{1}H resolution in HSQC spectra obtained using magnetic dilution are observed on the relevant ppm scale to be better resolved by a factor of ∼1.7 when ^{15}N decoupling is used instead of FSLG line narrowing. This is opposite of the trend observed at 500 MHz with 10 kHz MAS, where the ^{1}H resolution is reported to decrease by a factor of 1.5 on the ^{1}H ppm scale in a similar comparison.[6] Magnetic dilution with ^{15}N decoupling then provides the best combination of resolution and signal-to-noise, with the added bonus of requiring less total RF power be applied.

Much of this improved resolution can be attributed to the higher field operation here and the twice as fast MAS rate. However, it should also be noted that such results are only obtained if great care is taken to minimize t_1 noise by optimizing RF field stability and water suppression.

Pulse Sequences

The pulse sequence developed that best addresses these challenges in our hands is diagramed in Figure 1a. ^{15}N

(9) Martin, R. W., Paulson, E. K., and Zilm, K. W. *Rev. Sci. Instrum.* **2003**, *74*, 1−17.
(10) Bielecki, A.; Kolbert, A. C.; Levitt, M. H. *Chem. Phys. Lett.* **1989**, *155*, 341−346.
(11) vanRossum, B. J.; Forster, H.; deGroot, H. J. M. *J. Magn. Reson.* **1997**, *124*, 516−519.
(12) Vinogradov, E.; Madhu, P. K.; Vega, S. *Chem. Phys. Lett.* **1999**, *314*, 443−450.
(13) McDermott, A. E.; Creuzet, F. J.; Kolbert, A. C.; Griffin, R. G. *J. Magn. Reson.* **1992**, *98*, 408−413.
(14) Ishii, Y.; Ashida, J.; Terao, T. *Chem. Phys. Lett.* **1995**, *246*, 439−445.
(15) the reader should be aware that FSLG ^{1}H line widths reported as Hz in ref 6 are defined differently and include a correction for the 0.58 scaling factor.

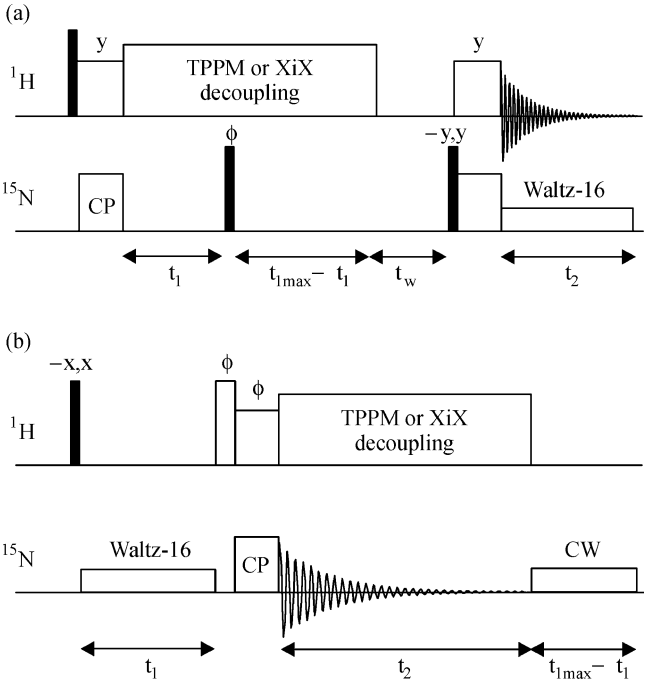

Figure 1. Pulse sequences used in this work. Solid bars represent $\pi/2$ pulses. Unless otherwise noted, pulse phases are set to *x*. (a) pulse sequence for ^{1}H detect ^{1}H/^{15}N solid-state HSQC spectroscopy. ^{1}H $\pi/2$ pulse lengths 2.4 μs. ^{15}N $\pi/2$ pulse 4.6 μs. TPPM decoupling performed at 100 kHz. ^{15}N CP transfers used ^{15}N RF field of ~55 kHz and ^{1}H RF field at ~75 kHz with a spin rate of ~20 kHz. t_{1max} is typically 40 ms, and $t_2 = 10$ ms. The phase ϕ of the first ^{15}N $\pi/2$ pulse is switched between $-y$ and x phases to aquire quadrature data in the indirect dimension. t_w typically set to 10 ms. ^{15}N RF level set to ~2.5 kHz during WALTZ-16 decoupling ^{1}H carrier frequency placed on the water resonance. ^{15}N $\pi/2$ pulse prior to final CP and receiver phase switched between y and −y on alternate scans. (b) pulse sequence for ^{15}N detect solid-state HSQC spectroscopy. RF levels and times for $\pi/2$ pulses, CP and decoupling as above. t_{1max} typically 10 ms. The ^{15}N frequency can be set to the middle of the amide band for decoupling during t_1, and then jumped to the center of the ^{15}N chemical shift range for CP during the ϕ phase ^{1}H spinlock pulse. This pulse serves to select the desired ^{1}H magnetization component. Typically, the ^{1}H carrier is placed on the water resonance, so quadrature data in t_1 is not required. The ^{1}H spinlock and the final CP usually then are set to *y* phase, but can also be phase stepped together in either a States or TPPI fashion if this is desired. The initial ^{1}H $\pi/2$ pulse and the receiver phase are switched between *x* and $-x$ on alternate scans.

magnetization is created using a fixed level CP of 150 μs. TEDOR transfers have also been used.[16,17] The latter give even more stable polarization transfer, but at the cost of 40% less signal. ^{15}N evolution proceeds under TPPM[18] or XiX[19] decoupling for t_1, and the desired component of the ^{15}N magnetization is projected onto the *z*-axis by a $\pi/2$ pulse. Decoupling is continued for a period $t_{1max} - t_1$, followed by a fixed delay for dephasing any remaining transverse ^{1}H magnetization. Transfer of the frequency labeled ^{15}N magnetization back to the ^{1}H is accomplished with a second ~150 μs CP. The precise length of this pulse is adjusted as part of the water suppression scheme, and the ^{1}H MAS signal finally acquired using WALTZ-16 ^{15}N decoupling.[5] Only a 2-step phase cycle is used, alternating the phase of the ^{15}N $\pi/2$ pulse by 180° on alternate scans. Figure 1b also depicts for comparison the pulse sequence used to obtain ^{15}N detected HSQC spectra, constructed following the same design principles.

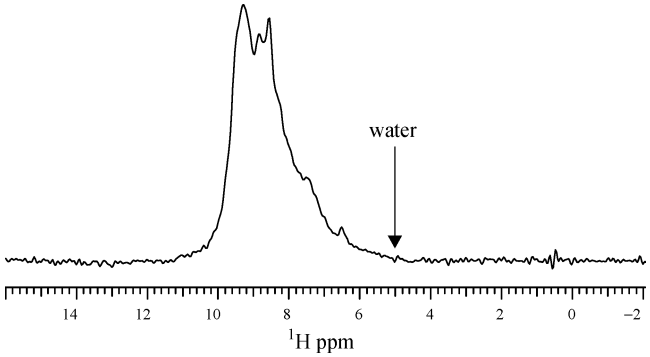

Figure 2. ^{1}H amide only spectrum obtained on ubiquitin nanocrystals prepared as described in the text. The pulse sequence in Figure 1a was used with t_1 set to zero. Two scans were acquired. The location where the water resonance would be observed is marked in the figure. This spectrum should be compared to that obtained with pulse field gradients and a 16 step phase cycle in ref 6 with 128 scans.

The pulse sequence in Figure 1a is deceptively simple yet effective in achieving suppression of the dominant ^{1}H water resonance. As noted elsewhere, this can be quite challenging. The excellent water suppression demonstrated in the amide only ^{1}H spectrum for ubiquitin shown in Figure 2 was achieved using the pulse sequence in Figure 1a with $t_1 = 0$ and only 2 scans. Prior to this work, pfgs and a 16-step phase cycle were required to achieve similar levels of water suppression with crystalline protein samples.[6] Keeping the proton decoupling on for t_{1max} effectively saturates the ^{1}H magnetization, and using the same time interval for every value of t_1 ensures that what water signal does remain, will always be the same. The subsequent ^{1}H spin lock pulse can then have its length, and if necessary its phase, adjusted to null any water magnetization echoing or relaxing prior to the final CP. Presumably incorporation of a pfg pulse during the dephasing delay would further improve performance, although the use of a homogeneity spoiling pulse did not. A second and just as important benefit to adopting the constant time RF scheme is that it greatly enhances overall system stability by keeping the thermal load experienced by the RF power amplifiers and the NMR probe constant throughout the experiment. Care is also taken to make certain that all amplifier noise blanking is done in a constant time manner as well. In addition to providing for superior water suppression, these precautions are essential for achieving sufficient stability in the polarization transfer to eliminate t_1 noise and to achieve resolution in the ^{15}N indirect dimension comparable to what is possible in ^{15}N detect mode.

Even with this level of experimental care, optimal performance requires careful alignment of the spectrometer on the protein sample itself. Both CP levels must be independently matched, and the decoupling parameters optimized on the experiment as performed. Experimentally, it is observed that ^{1}H decoupling performance as measured by ^{15}N peak height is a sensitive and highly nonlinear function of the decoupling level. Parameters determined in a direct ^{15}N detection experiment are then not sufficiently accurate to be transferred to the ^{1}H detect experiment if the RF power amplifier droops even only 1% over a 40 ms interval.

(16) Hing, A. W.; Vega, S.; Schaefer, J. *J. Magn. Reson.* **1992**, *96*, 205−209.
(17) Schnell, I.; Langer, B.; Sontjens, S. H. M.; van Genderen, M. H. P.; Sijbesma, R. P.; Spiess, H. W. *J. Magn. Reson.* **2001**, *150*, 57−70.
(18) Bennett, A. E.; Rienstra, C. M.; Auger, M.; Lakshmi, K. V.; Griffin, R. G. *J. Chem. Phys.* **1995**, *103*, 6951−6958.
(19) Detken, A.; Hardy, E. H.; Ernst, M.; Meier, B. H. *Chem. Phys. Lett.* **2002**, *356*, 298−304.

Experimental Section

Perdeuterated ^{15}N enriched ubiquitin was prepared in *E. coli* BL21star cells using a plasmid obtained from Prof. Tracy Handel, U. C. Berkeley. The cells were grown in M9 minimal media containing 1 g/liter $^{15}NH_4Cl$ and 2 g/liter U−D_6-glucose made in 98% D_2O. Isotopically enriched compounds were obtained from Cambridge Isotope Laboratories, Inc. The protein was purified using reversed phase HPLC and the identity and isotope incorporation was confirmed using electrospray mass spectrometry. Ubiquitin enriched solely in ^{15}N was provided by VLI Research Inc., Malvern, PA. Ubiquitin nanocrystals were prepared using poly(ethylene glycol) (PEG) or perdeuterated 2-methyl-2,4-pentanediol (MPD) following protocols detailed elsewhere.[20,21] Several milligrams of nanocrystals were packed into 2.5 mm zirconia MAS rotors using precautions that have been described to ensure long-term retention of sample hydration levels.[9]

All NMR spectroscopy was carried out using a Varian Inc. Inova instrument operating at 799.59 MHz for ^1H. The spectrometer is equipped with a high power cavity tuned vacuum tube ^1H frequency amplifier, and uses a $^1H/^{13}C/^{15}N$ MAS probe of our own design. The availability of a low noise Varian preamplifier with an actively switched transmit/receive duplexer capable of handling the full ^1H decoupling power during ^{15}N evolution was especially critical to the performance of the ^1H detect experiment. Pulse parameters are detailed in the figure captions. Power levels required and variable temperature performance of the probe used have been described in detail previously.[9] Samples were spun at ∼20 kHz and kept cooled to ∼278 K. Initial spectrometer alignment was performed using a sample of $^{13}C/^{15}N$ enriched glycine, and subsequent fine-tuning of all parameters performed on the protein samples themselves. Chemical shifts were referenced by relating the ^{13}C chemical shifts of external adamantane[22] to the ^1H and ^{15}N chemical shift scales.[23,24]

NMR Results and Discussion

Figure 3 compares ^{15}N and ^1H detect $^1H/^{15}N$ HSQC spectra for uniformly ^{15}N and ^2D enriched ubiquitin nanocrystals precipitated with MPD and acquired using the NMR pulse sequences shown in Figure 1. The spectrum in Figure 3a is the best ^{15}N detected HSQC acquired to date on this sample preparation. This is compared to an optimized ^1H detect spectrum on another sample in Figure 3b. Both data sets were apodized with standard sine-bell resolution enhancement windowing functions to generate the contour maps shown, and indicate the liquidlike resolution that can be achieved. Skyline projections are provided to roughly indicate the level of signal-to-noise in the 2D planes. The pair of 2D contour maps display just over 50 separate cross-peaks each, as counted by a computer automated peak pick. The ^1H detect experiment used only 2 scans for each of the 192 complex points acquired. With a recycle delay of 1 s these data took only 13 min to acquire after steady state was established.

Much more site to site variation in the intensity of the peaks in the 2D map is observed in the ^1H detect experiment. In part, this is due to differential cross polarization efficiency, which is magnified in the ^1H detect experiment as two CP steps are required. This is also a result of more variation in the widths of the indirectly detected ^{15}N line shapes, which in part is a consequence of the greater difficulty encountered in optimizing the ^1H decoupling in the indirect dimension. In general, we find that the resolution in the indirect dimension of either experiment is close to, but never quite as good as, the best that can be achieved in the complementary experiment where that nucleus is directly detected. Drift in either the decoupling power or in the CP condition can easily lead to a doubling of the line widths in the indirect dimension.

A higher signal-to-noise ^{15}N detect spectrum was acquired for measurement of line widths and for comparing sensitivity to the ^1H detect spectrum in Figure 3b. This experiment used the same sample as in Figure 3b, but 8 times as many scans. Slices along the ^1H dimension from both are compared in Figure 4 for the two positions indicated in Figure 3b. We measure these widths using no apodization of the data, and only compare slices with close to the same number of points per Hz. For either direct or indirectly detected experiments, the ^1H line widths lie in a range from 0.17 to 0.39 ppm, i.e., from 140 to 310 Hz, with the average close to 0.22 ppm, or 180 Hz. The ^1H lines observed in the present work are actually narrower than the ^{15}N lines on the ppm scale, which at ∼35 Hz are ∼0.44 ppm fwhm.

The relative merits of the line narrowing provided by 20 kHz MAS, FSLG, or ^{15}N decoupling were most thoroughly investigated on PEG precipitated deuterated nanocrystals. Focusing on a single line at $^{15}N/^1H$ coordinates of 127.3/9.5 ppm, we observe a ^1H line width of 280 Hz (0.35 ppm) with MAS alone that narrows to 160 Hz (0.2 ppm) when WALTZ-16 ^{15}N decoupling is applied. The same line with FSLG line narrowing but without ^{15}N decoupling is measured to be 160 Hz, or 0.35 ppm when the FSLG scaling factor is taken into account. This latter result agrees well with observations made at 500 MHz, where ^1H line widths of 0.35 ppm were also reported using FSLG alone.[6] However, in that work when ^{15}N decoupling was applied without FSLG, the line widths *increased* by a factor of 1.5 in ppm. This is opposite to the result obtained here at 800 MHz and a 20 kHz MAS rate, where the line widths *decrease* by a factor of 1.7. Overall the resolution in the comparable experiments improves by a factor of 2.6 on moving to the higher field and faster MAS rate conditions.

The signal-to-noise advantage of the ^1H detect experiment is obvious. In Figure 4 the ^{15}N detect ^1H slices were scaled so that the peak heights in Figure 4a and 4b would match. This results in a noise amplitude that is conservatively measured as 2.5 times greater than in the ^1H detect experiment. Taking into account the $\sqrt{8}$ advantage the greater number of scans provides, the improvement in signal-to-noise provided on this sample by ^1H detection is a factor of 7. This agrees with eq 3 taking the average ^{15}N line width to be 35 Hz and the average ^1H line width as 180 Hz, resulting in a predicted factor of 7.1.

Just exactly how much advantage is provided by the ^1H detect experiment depends on sample quality and how well the experiments are optimized. The sample used to acquire the ^{15}N detect spectrum in Figure 3a has ^{15}N lines closer to 25 Hz fwhm on average, a consequence of a better sample preparation and the sample responding better to ^1H decoupling. Both types of experiments would benefit from better ^1H decoupling to achieve more uniformly narrow ^{15}N lines. In general ^1H decoupling for ^{15}N seems to be experimentally more demanding, with the optimum parameters occupying a narrower space, than is our experience with ^{13}C. Although there are reasons to expect this

(20) Martin, R. W.; Zilm, K. W. *J. Magn. Reson.* **2003**, *165*, 162−174.
(21) Igumenova, T. I. *Assignment of Uniformly Carbon-13-Enriched Proteins and Optimization of their Carbon Line Shapes*; Columbia University: New York, 2003.
(22) Morcombe, C. R.; Zilm, K. W. *J. Magn. Reson.* **2003**, *162*, 173−180.
(23) Harris, R. K.; Becker, E. D.; De Menezes, S. M. C.; Goodfellow, R.; Granger, P. *Pure Appl. Chem.* **2001**, *73*, 1795−1818.
(24) Wishart, D. S.; Bigam, C. G.; Yao, J.; Abildgaard, F.; Dyson, H. J.; Oldfield, E.; Markley, J. L.; Sykes, B. D. *J. Biomol. NMR* **1995**, *6*, 135−140.

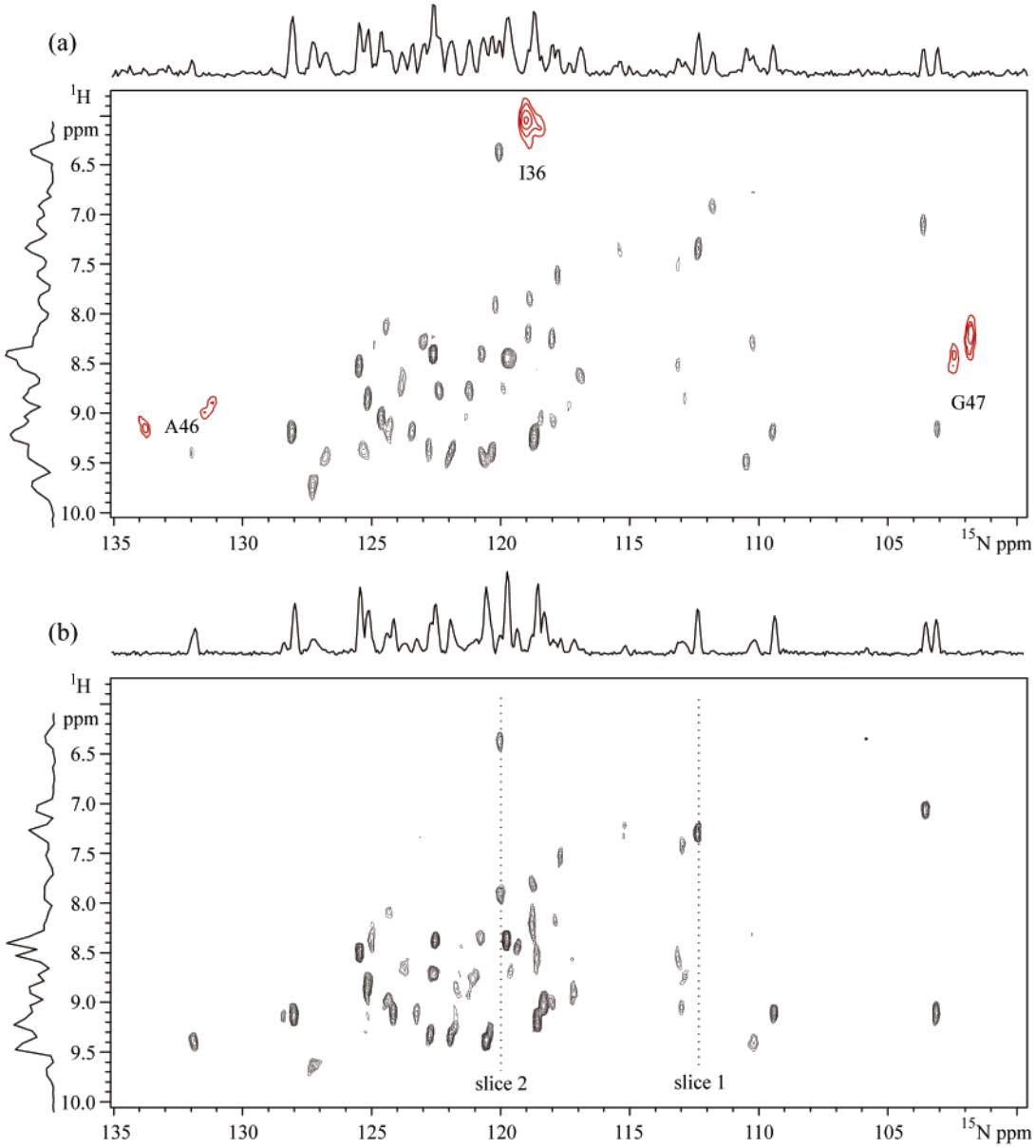

Figure 3. Comparison of ^{1}H/^{15}N HSQC spectra taken on MPD ubiquitin nanocrystals. (a) Exceptional example of an ^{15}N detect spectrum. 128 t_1 points acquired, using a dwell time of 52 μs in t_1. ^{1}H carrier placed on the water resonance. 16 scans per t_1 point, 1 s recycle delay. Spectral width in the ^{15}N dimension set to 25 kHz. Unfortunately, this particular sample was inadvertently melted and subsequent preparations have not quite matched the ^{15}N resolution displayed here. The peaks observed for G47, A46, and I36 in a sample of PEG precipitated ubiquitin nanocrystals are shown as red insets. One lower contour was used for the A46 peaks inset as they are low intensity. (b) ^{1}H detect spectrum of MPD ubiquitin nanocrystals using 2 scans per 192 complex t_1 points with a dwell time of 208 μs in t_1. Pulse sequence parameters for both sets of data as described in the caption to Figure 1.

would be the case,[25] a general solution to providing efficient and robust ^{1}H decoupling for ^{15}N MAS ssNMR seems to remain a challenge.

In addition to this particular preparation, we have also acquired solid state ^{1}H/^{15}N HSQC spectra for ubiquitin nanocrystals using PEG as the crowding agent.[20] This results in another crystal form, with a much larger unit cell and a doubling in the number of lines. This presumably is a consequence of the presence of at least two magnetically inequivalent molecules in the asymmetric unit. The different shifts are then for ubiquitin molecules with subtly different structures. Resolution in the 2D plane is comparable for this sample, but with double the number of resonances the central portion of the 2D map is significantly more crowded. The peaks for G47, A46, and I36 are still clear outliers, and are easily assigned by analogy to the known solution NMR shifts and the assigned ^{15}N shifts[21] for the MPD crystallized form. These peaks for the PEG nanocrystals are depicted as colored insets in Figure 3a to show their relation to the peaks observed in the MPD form. Table 1 collects these shifts, referenced to DSS with a precision of $\pm$0.03 ppm.[22,23] They vary over 0.5 ppm in the ^{1}H dimension, and up to 1.3 ppm in ^{15}N shift for any single amino acid center, and are quite different from those measured in solution.[26] Once X-ray diffraction data is available for these new polymorphs, it will be interesting to see how the shifts correlate with variations in the X-ray determined crystal structures. Such comparisons in

(25) Ernst, M.; Bush, S.; Kolbert, A. C.; Pines, A. *J. Chem. Phys.* **1996**, *105*, 3387−3397.

(26) Wang, A. C.; Grzesiek, S.; Tschudin, R.; Lodi, P. J.; Bax, A. *J. Biomol. NMR* **1995**, *5*, 376−382.

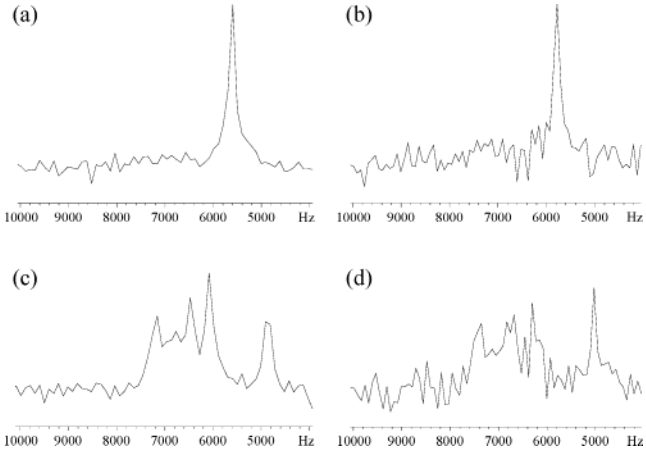

Figure 4. Assessment of ^{1}H line widths and relative sensitivity of ^{1}H detect and ^{15}N detect HSQC spectra. (a) ^{1}H detect and (b) ^{15}N detect slices showing the ^{1}H spectra obtained at the position corresponding to slice 1 in Figure 3b. (c) ^{1}H detect and (d) ^{15}N detect slices depicting the ^{1}H spectra obtained at the position corresponding to slice 2 in Figure 3b. Although the ^{15}N detect spectra were acquired using 8× as many scans, the noise level is over 2.5× as large. In each case, the data sets Fourier transformed contained 10 ms of evolution for ^{1}H, and 40 ms of evolution for ^{15}N. Since the direct and indirect ^{1}H dwell times were not the same, the data table was zero filled to result in spectra with as close to the same digital resolution as possible.

Table 1. Outlying Ubiquitin Solid State and Solution NMR Shifts

sample	A46 ^{15}N	A46 ^{1}H	G47 ^{15}N	G47 ^{1}H	I36 ^{15}N	I36 ^{1}H
MPD crystals	132.0	9.4	103.0	9.2	120.0	6.4
PEG crystals, molecule 1	133.1	9.1	101.7	8.2	118.9	6.0
PEG crystals, molecule 2	133.1	8.9	102.4	8.4	118.5	6.1
solution phase	132.20	8.81	102.34	8.13	119.88	6.15

Notes: ^{1}H shifts in ppm from DSS as described in ref 22 and 23. ^{15}N shifts referenced according to ref 24. Solution shifts from ref 26. Assignment of the pairs of shifts in the PEG crystals to particular molecules is arbitrary at this time.

combination with chemical shift calculations of the type already successfully applied to studying dynamic protein structures in solution[27] will undoubtedly provide a valuable new experimental connection between time averaged solution NMR structures and chemical shifts and X-ray crystal structures via ssNMR.

Conclusions

We have reported a new ^{1}H detected ^{1}H/^{15}N HSQC experiment for studying nanocrystalline proteins. Using standard ^{15}N and ^{2}D enrichment to affect magnetic dilution of the ^{1}H nuclei, MAS at 20 kHz is sufficient to produce ^{1}H line widths of only 0.22 ppm. This provides useful dispersion in the ^{1}H dimension in MAS ssNMR of proteins. Spectral resolution and the quality of water suppression are both linked to operating in a manner that maximally enhances spectrometer stability, an area where further technical innovations would be a welcome improvement. The pulse sequence described herein improves over previous methods by reducing the phase cycle a factor of 8 and eliminating the need for a pfg coil in the MAS probe. An important observation here is the identification of the need for constant power operation in maximizing resolution. The shortening of the experiment to a 2 step cycle makes it a much better building block for incorporation into 3D ssNMR methods for spectral assignment and obtaining tertiary structural constraints.

The ability to resolve ^{1}H and ^{15}N chemical shifts for different protein polymorphs and different protein molecules in the same unit cell by ssNMR is an important step toward directly linking NMR chemical shifts to protein structure variations. On the practical side, this highlights the potential of ssNMR as an analytical tool for characterizing distinct forms of a protein in solid-phase preparations, with potential utility in pharmaceutical applications.[20] The broader impact of this observation, however, is the recognition that sufficient accuracy and resolution is now attainable by ssNMR to make possible correlation of protein chemical shifts with actual X-ray crystal structures for the same crystal form. Because the solid state is less influenced by large scale molecular dynamics, structure-shift relations determined in this manner are likely to be more direct, and should provide a better foundation on which solution chemical shifts can be related to protein structure and dynamics in the solution phase.

In addition to being a significant technical achievement on the path to making ssNMR methods more applicable to problems in structural biology, this work represents a turning point in terms of ssNMR sensitivity required to study large molecules. The work carried out here used a sample occupying a volume of 6.5 microliters and containing approximately 4 milligrams of protein, i.e., only 500 nanomoles. A not atypical solution NMR study might use 300 microliters of a 1 millimolar solution, or about 2/3 the amount of protein. Even with this small sample, the sensitivity of the experiment is such that signal averaging beyond the 2-step phase cycle is not required. From the solid-state NMR spectroscopist's perspective this is an important milestone. We expect methods of the type presented here in combination with improvements in ssNMR hardware will make possible the adaptation of ssNMR methods to the solution of an ever wider range of problems in biophysical chemistry.

Acknowledgment. This work was supported in part by the Wm. M. Keck Foundation and ExxonMobil. C.R.M. gratefully acknowledges the support of a NSERC post-graduate fellowship. The authors gratefully acknowledge A. Brooke and A. Schwartz of Varian Inc. for assistance in acquiring the low noise ^{1}H preamplifier with high power handling capabilities.

JA037315+

(27) Pearson, J. G.; Le, H. B.; Sanders, L. K.; Godbout, N.; Havlin, R. H.; Oldfield, E. *J. Am. Chem. Soc.* **1997**, *119*, 11 941−11 950.